

The synthesis of crystalline SnO₂ whiskers via a metalorganic chemical vapor deposition process

Myung Ho Kong^a, Yong Jung Kwon^b, Dong Sub Kwak^b, Tran Van Khai^b, Jinho Ahn^b, Kwang Bo Shim^b, Chongmu Lee^c, Inpil Kang^d, No-Hyung Park^e, Dae-Sup So^f, Joon Woo Lee^f and Hyoun Woo Kim^{b,*}

^aKorea Institute of Materials Science, Changwon, Gyeongnam 641-831, Republic of Korea

^bDivision of Materials Science and Engineering, Hanyang University, Seoul 133-791, Republic of Korea

^cDivision of Materials Science and Engineering, Inha University, Incheon 402-751, Republic of Korea

^dDepartment of Mechanical and Automotive Engineering, Pukyong National University, Busan 608-739, Republic of Korea

^eDepartment of Textile Convergence of Biotechnology & Nanotechnology, Korea Institute of Industrial Technology, Gyeonggi-do 426-910, Republic of Korea

^fNational Nanotechnology Policy Center, Korea Institute of Science and Technology Information, Seoul 130-741, Republic of Korea

We demonstrate the synthesis of one-dimensional (1D) structures of tin oxide (SnO₂) by a reaction of a tetramethyltin (Sn(CH₃)₄) and oxygen (O₂) mixture at 800 °C. Scanning electron microscopy showed that the morphology of the products was changed by varying the growth temperature. 1D and 2D structures were favored at 800 and 600 °C, respectively. We suggest the associated mechanisms by which the temperature controlled the morphology. X-ray energy dispersive spectroscopy revealed that the products contained elements of Sn and O. X-ray diffraction, selected area electron diffraction, and lattice-resolved transmission electron microscopy indicated that the SnO₂ obtained were crystalline with a tetragonal structure. The Raman spectra exhibited three normal interior phonon modes corresponding to the tetragonal rutile SnO₂ structure. The intensity of yellow photoluminescence emission increased with an increasing growth temperature in the range of 700–800 °C.

Key words: Nanostructures, Chemical synthesis, Transmission electron microscopy.

Introduction

One-dimensional (1D) nanostructures are of great interest because of their novel physical and chemical properties [1-16], tremendous efforts have focused on the synthesis and characterization of these materials over the past several years. Tin oxide (SnO₂) is a typical n-type semiconductor with a wide direct band gap of 3.6 eV. Due to its peculiar and useful properties, 1D nanostructures of SnO₂ have applications in several technological fields, including dye-sensitized solar cells [17], gas sensors [18, 19], ethanol sensors [20], lithium ion batteries [21], and photoconductors [22].

Owing to the scientific and technological importance of 1D SnO₂ nanostructures, many research groups have fabricated them using a variety of techniques. Thanasanvorakun et. al synthesized SnO₂ nanowires by a carbothermal reduction process using SnO as the starting material and CuO as the catalyst [23]. Wang et al. fabricated SnO₂ nanowires by oxidizing SnO nanoparticles in a NaCl flux [24]. In addition, SnO₂ nanowires and nanobelts have been synthesized by heating Sn powders [25-27].

Although numerous papers have been published on the growth of SnO₂ thin films by metalorganic CVD (MOCVD) [28-31], there has been no report on the fabrication of SnO₂ 1D nanostructures by such a method. The MOCVD method has several advantages. First, the amount of source material can be precisely controlled and thus abrupt interfaces can be formed, making the product suitable for ultra large scale integrated circuit (ULSI) fabrication. Second, only one heating zone is required, which achieves a simple design of the equipment and mass production. Third, controlling the process is easy, with the growth rate being extensively varied. In this paper, we report the fabrication of crystalline 1D SnO₂ nanomaterials using a reaction of a tetramethyltin (Sn(CH₃)₄) and O₂ mixture. In addition, we investigated the structural and optical properties.

Experimental

The deposition of the SnO₂ products was carried out using a MOCVD system. A schematic illustration of the MOCVD reactor used in our experiments was previously reported [32]. We used p-type Si(100) substrates as starting materials, onto which a layer of Au (about 3 nm) was deposited by radio frequency magnetron sputtering. Sn(CH₃)₄ and O₂ were used as the Sn and O sources, respectively, with Ar as the

*Corresponding author:
Tel : +82-2-2220-0382
Fax: +82-2-2220-0389
E-mail: hyounwoo@hanyang.ac.kr

carrier gas. The MO bubbler was maintained at 5 °C and its vapor was transported into a reactor by Ar. High purity O₂ was injected using a separate delivery line into the reactor as the oxidant. The Ar and O₂ gas flow rates, respectively, were set to 30 standard cubic centimetres per minute (sccm) and 10 sccm, with the growth pressure at 133 Pa. The deposition time was approximately 10 minutes. To investigate the effect of temperature, the experiments were performed at different substrate temperatures at the central region ranging from 600 to 800 °C.

The samples were analyzed by X-ray diffraction (XRD, X'pert MRD-Philips) using CuK_α radiation ($\lambda = 0.154056$ nm), scanning electron microscopy (SEM, Hitachi S-4200), and transmission electron microscopy (TEM, Philips CM-200) with energy-dispersive X-ray (EDX) spectroscopy attached. Micro-Raman spectra were obtained using a Renishaw Raman spectromicroscope at room temperature in the open air. An He-Ne laser beam with a wavelength of 633 nm was used for Raman excitation. PL measurements were performed using a He-Cd laser line (325 nm, 55 mW) as the excitation source at room temperature at KBSI.

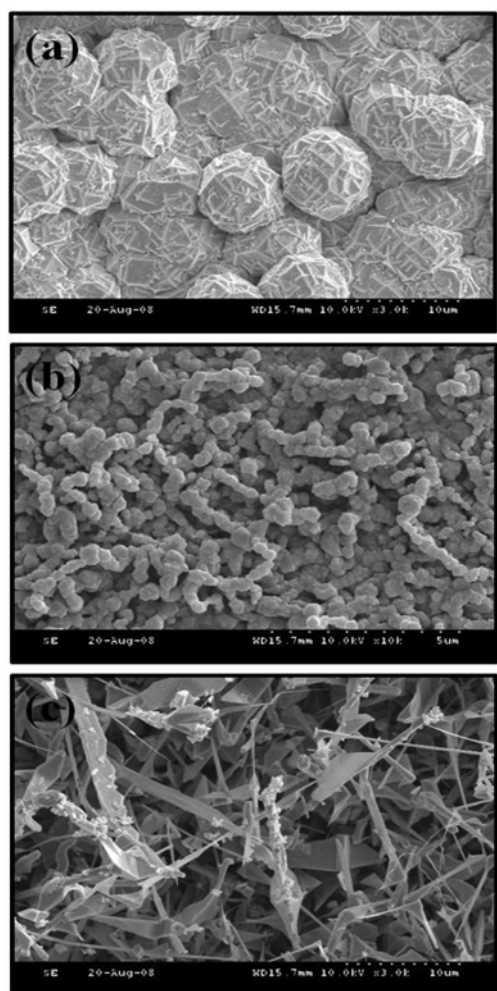


Fig. 1. Plan-view SEM images of the products at substrate temperatures of (a) 600 °C, (b) 700 °C, and (c) 800 °C.

Results and Discussion

Figs. 1a, 1b, and 1c show plan-view SEM images of the deposits, with substrate temperatures of 600, 700, and 800 °C, respectively. The 600 °C-grown product corresponds to the film-like structure (Fig. 1a), whereas the 800 °C-grown product is comprised of 1D structures. It is noteworthy that the 700 °C-grown product is an intermediate state between the products fabricated at 600 °C and 800 °C, indicating that this material consists of film-like structures with aggregates of relatively thick 1D structures being generated on the top surface. Accordingly, we observe that the substrate temperature significantly influences the product morphology, in which thin 1D structures are favored at higher temperature. Figs. 2a and 2b display the typical XRD spectra of the products fabricated at 700 °C and 800 °C, indicating that the XRD spectra are not dependent on the temperature in the range of 700-800 °C. All recognizable reflection peaks including (110), (101), (200), (111), (211), (220), (002), (310), (112), (301), (112), (301), (202), and (321) correspond to the tetragonal rutile SnO₂ structure with lattice constants $a = 4.738$ Å and $c = 3.187$ Å (JCPDS: 41-1445).

By means of the EDX analysis, we observe that the whiskers consist of only Sn and O elements, regardless of position, from the stems to the ends (Fig. 3). The C peaks and Cu peaks arose from a TEM Cu grid coated with amorphous carbon film on which the whisker was placed. This revealed that the as-synthesized structure comprises Sn and O elements. Fig. 4a shows a representative TEM image of a single whisker. It exhibits an almost smooth surface with its width being reduced along the length direction. A selected area electron diffraction (SAED) pattern, with the incident electron beam parallel to the [011] direction,

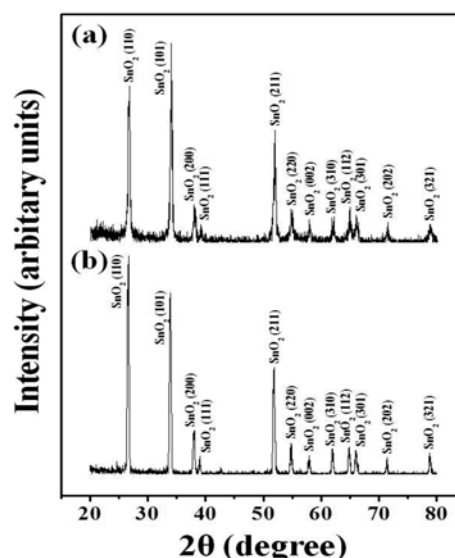


Fig. 2. X-ray diffraction pattern recorded from the products synthesized at (a) 700 °C and (b) 800 °C.

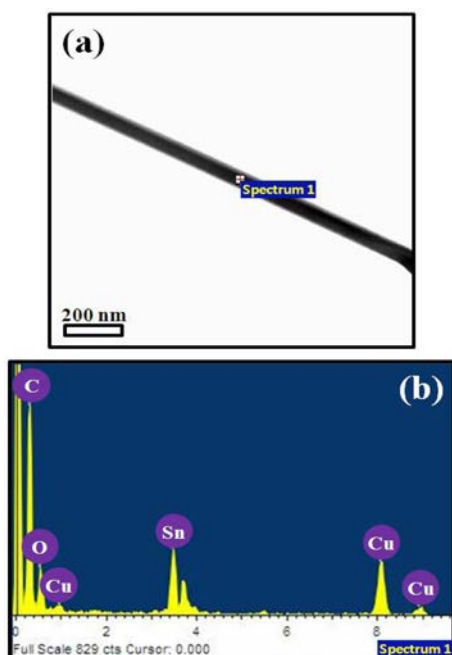


Fig. 3. (a) Typical whisker and (b) corresponding EDX spectrum.

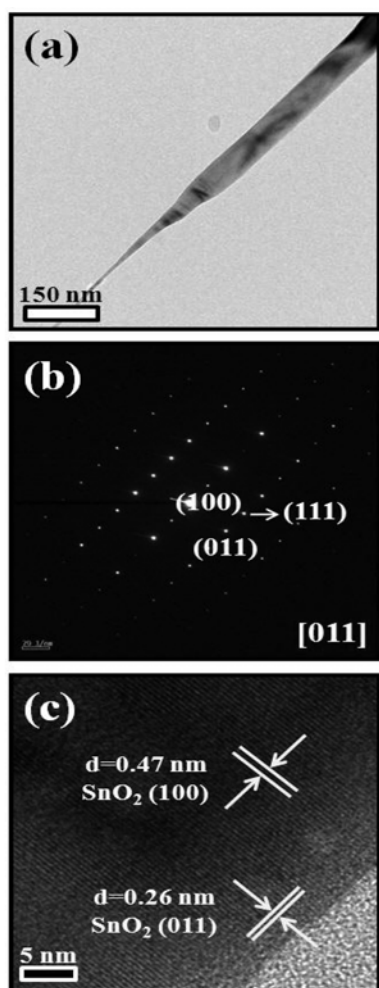


Fig. 4. (a) Low-magnification TEM image of a whisker. (b) Corresponding SAED pattern. (c) Lattice resolved TEM image near the surface of a whisker.

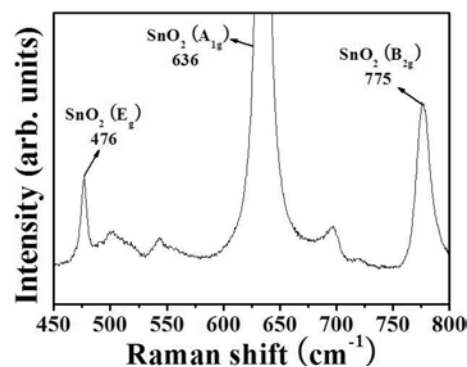


Fig. 5. Raman spectrum of the 800 °C-grown whiskers.

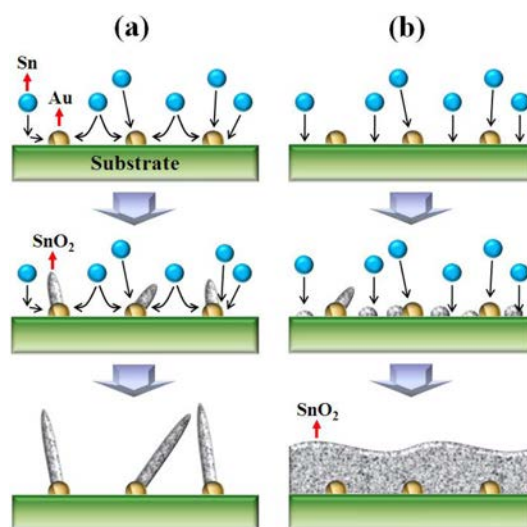


Fig. 6. Schematic outline of the growth of products at (a) 800 °C and (b) 600 °C.

is presented in Fig. 4b. The reflections in the SAED pattern correspond to the lattice planes of tetragonal SnO₂, indicating that the whisker is crystalline. Fig. 4c shows the visible lattice fringes of a high resolution TEM (HRTEM) image recorded near the edge of the whisker in Fig. 4a. The interplanar spacings are about 0.47 and 0.26 nm, corresponding to the (100) and (011) planes of tetragonal SnO₂, respectively. Fig. 5a shows the Raman spectrum of the whiskers fabricated at 800 °C. The lines at frequencies of 476, 636, and 775 cm⁻¹, are observed, corresponding to three normal interior phonon modes, E_g, A_{1g}, and B_{2g} respectively. They usually appear in large single crystals or bulk polycrystalline SnO₂ materials [33-35], confirming the tetragonal rutile structure of the SnO₂ whiskers.

In the present study, the Sn(CH₃)₄ is decomposed at the growth temperature and Sn-related vapors can be generated. The Sn-related vapor which is in the ambient or adsorbed on the substrate surface combines with oxygen gas, resulting in the formation of solid SnO₂ on the substrate. SEM and TEM analyses (not shown here) coincidentally indicated that the whisker tips were free of Au-related particles, excluding the tip-growth vapor-liquid-solid (VLS) mechanism. Since the

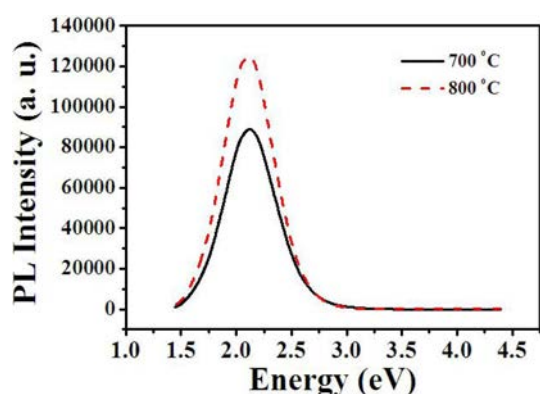


Fig. 7. Room-temperature PL spectra of the products synthesized at 700 °C and 800 °C.

Au on the substrate played a catalytic role in forming nanowires (in preliminary experiments, Si substrates without the Au layer did not produce thin 1D nanostructures), the dominating mechanism should be a base-growth process. In the present study, the 1D and 2D structures are favored at 600 and 800 °C, respectively. This indicates that the growth of 1D structures is controlled by the diffusion of Sn-related species into Au particles to supersaturate the melt. At a high temperature of 800 °C, the Sn diffusion is activated and most Sn-species can be alloyed with the Au particles, producing the individually grown 1D structures (Fig. 6a). On the other hand, at a low temperature of 600 °C, the Sn-related species are nearly omnipresent on the substrate surface. Accordingly, many nuclei form over the entire substrate surface. The nuclei coalesce to form film-like structures (Fig. 6b).

Fig. 7 gives the PL spectra of the products grown at 700 and 800 °C, respectively, being centered at about 2.1 eV in the yellow region. The excitation energy of the He-Cd laser ($\lambda_{\text{ex}} = 325 \text{ nm} = 3.82 \text{ eV}$) is high enough to pump carriers to the excited states, overcoming the reported band gap of SnO₂ (3.6 eV) [36]. Yellow luminescence is known to be associated with O vacancies or Sn interstitials that have been generated during the synthesis process [37, 38]. Although the shape of the PL spectra for the two samples is similar, we reveal that the overall emission intensity becomes stronger with an increasing synthesis temperature. One possibility is that the increased amount of defects, such as O vacancies or Sn interstitials in a higher-temperature process, helps to increase the PL emission intensity. On the other hand, the 800 °C-grown whiskers have a higher surface-to-volume ratio than the 700 °C-grown structures. The other possibility is that the larger surface area will contribute to the intensification of PL emission.

Conclusions

We have achieved the growth of 1D SnO₂ nanomaterials by means of the MOCVD technique. SEM images indicate that the product morphology is

significantly dependent on the substrate temperature, in which thin 1D structures are favored at a higher temperature. XRD spectra, EDX spectra, SAED patterns, and lattice-resolved TEM images coincidentally reveal that the synthesized whiskers correspond to a tetragonal rutile SnO₂ structure. The Raman spectra exhibit three normal interior phonon modes, E_g, A_{1g}, and B_{2g}, confirming the tetragonal rutile structure of the SnO₂ whiskers. We compared the PL spectra of the 700 °C- and 800 °C-synthesized products. Although the peak position was not changed, the intensity of the yellow emission was enhanced by increasing the substrate temperature. This observation is attributed to the temperature-induced increase of defects and/or an increase of the surface-to-volume ratio of the products.

Acknowledgements

This work was supported by the research fund of Hanyang University (HY-2011-20110000000434).

References

- H.Y. Yang and T.W. Kim, *J. Ceram. Proc. Res.* 11 (2010) 769-772.
- C.S. Lim, J.H. Ryu, D.-H. Kim, S.-Y. Cho and W.-C. Oh, *J. Ceram. Proc. Res.* 11 (2010) 736-741.
- F.A. Sheikh, M.A. Kanjwari, H. Kim, D.R. Pandeya, S.T. Hong and H.Y. Kim, *J. Ceram. Proc. Res.* 11 (2010) 685-691.
- K.-S. Yun and C.-J. Park, *Electron. Mater. Lett.* 6 (2010) 173-176.
- C. Hong, H. Kim, H.W. Kim and C. Lee, *Met. Mater. Int.* 16 (2010) 311-315.
- H.W. Kim, H.S. Kim, M.A. Kebede, H.G. Na and J.C. Yang, *Met. Mater. Int.* 16 (2010) 77-81.
- Y.-S. Kim, K.-C. Kim and T.-W. Hong, *Met. Mater. Int.* 16 (2010) 225-228.
- D.Y. Lee, M.-H. Lee, N.-I. Cho, B.-Y. Kim and Y.-J. Oh, *Met. Mater. Int.* 16 (2010) 453-457.
- C.M. Choi, Y.C. Yoon, D.H. Hong, K. S. Brammer, K.B. Noh, Y. Oh, S.H. Oh, F.E. Talke and S.H. Jin, *Electron. Mater. Lett.* 6 (2010) 59-65.
- S.G. Shin, *Electron. Mater. Lett.* 6 (2010) 65-71.
- S. Iijima, *Nature* 354 (1991) 56-58.
- E.W. Wong, P.E. Sheehan and C.M. Lieber, *Science* 277 (1997) 1971-1975.
- J.T. Hu, T.W. Odom and C.M. Lieber, *Acc. Chem. Res.* 32 (1999) 435-445.
- Z.W. Pan, Z.R. Dai and Z.L. Wang, *Science* 291 (2001) 1947-1949.
- L.F. Dong, J. Jiao, D.W. Tuggle, J. Petty, S.A. Elliff and M. Coulter, *Appl. Phys. Lett.* 82 (2003) 1096.
- Z. Pan, H.-L. Lai, F.C.K. Au, X. Duan, W. Zhou, W. Shi, N. Wang, C.-S. Lee, N.-B. Wong, S.-T. Lee and S. Xie, *Adv. Mater.* 12 (2000) 1186-1190.
- S. Gubbala, V. Chakrapani, V. Kumar and M.K. Sunkara, *Adv. Funct. Mater.* 18 (2008) 2411-2418.
- N.S. Ramgir, I.S. Mulla and K.P. Vijayamohanam, *Sens. Actuators B: Chem.* 107 (2005) 708-715.

19. A. Kolmakov, D.O. Klenov, Y. Lilach, S. Stemmer and M. Moskovits, *Nano Lett.* 5 (2005) 667-673.
20. N. Van Hieu, H.-R. Kim, B.-K. Ju and J.-H. Lee, *Sens. Actuators B: Chem.* 133 (2008) 228-234.
21. M.-S. Park, G.-X. Wang, Y.-M. Kang, D. Wexler, S.-X. Dou and H.-K. Liu, *Ang. Chem., Int. Ed.* 46 (2007) 750-753.
22. S. Mathur, S. Barth, H. Shen, J.C. Pyun and U. Werner, *Small* 1 (2005) 713-717.
23. S. Thanasanvorakun, P. Mangkornong, S. Choopun and N. Mangkornong, *Ceram. Int.* 34 (2008) 1127-1130.
24. W. Wang, J. Niu and L. Ao, *J. Cryst. Growth* 310 (2008) 351-355.
25. M.-R. Yang, S.-Y. Chu and R.-C. Chang, *Sens. Actuators B: Chem.* 122 (2007) 269-273.
26. H.W. Kim and S.H. Shim, *J. Korean Phys. Soc.* 47 (2005) 516-519.
27. S. Luo, J. Fan, W. Lu, M. Zhang, Z. Song, C. Lin, X. Wu and P.K. Chu, *Nanotechnology* 17 (2006) 1695-1699.
28. C.N. Luan, J. Ma, Z. Zhu, L.Y. Kong and Q.Q. Yu, *J. Cryst. Growth* 318 (2011) 599-601.
29. S.Y. Zhao, P.H. Wei and S.H. Chen, *Sens. Actuators B-Chemical* 62 (2000) 117-120.
30. X.J. Feng, J. Ma, F. Yang, F. Ji, C. Luan and H.L. Ma, *J. Cryst. Growth* 310 (2008) 295-298.
31. S.W. Lee, P.P. Tsai and H.D. Chen, *Sens. Actuators B: Chem.* 41 (1997) 55-61.
32. H.W. Kim and N.H. Kim, *Appl. Phys. A* 81 (2005) 763-765.
33. Y. Liu and M. Liu, *Adv. Funct. Mater.* 15 (2005) 57-62.
34. L. Abello, B. Bochu, A. Gaskov, S. Koudryavtseva, G. Lucazeau and M. Roumyantseva, *J. Solid State Chem.* 135 (1998) 78-85.
35. A. Dieguez, A. Romano-Rodriguez, A. Vila and R. Morante, *J. Appl. Phys.* 90 (2001) 1550-1557.
36. T.L. Credelle, C.G. Fonstad and R.H. Rediker, *Bull. Am. Phys. Soc.* 16 (1971) 519.
37. J.Q. Hu, Y. Bando, Q. Liu and D. Golberg, *Adv. Funct. Mater.* 13 (2003) 493-496.
38. B. Cheng, J. M. Russell, W. Shi, L. Zhang and E.T. Samulski, *J. Am. Chem. Soc.* 126 (2004) 5972-5973.